CAAP Annual Report

Date of Report: *09/30/2024*

Prepared for: *U.S. DOT Pipeline and Hazardous Materials Safety Administration*

Annual Period: **From** *(09/01/2023)* **to** *(09/30/2024)*

Contract Number: # 693JK32350005CAAP

Project Title: Development of a Framework for Assessing Cathodic Protection (CP) Effectiveness in Pipelines Based on Artificial Intelligence (AI)

Prepared by: TEES (Texas A&M Engineering Experiment Station)

Prof. Homero Castaneda

The University of Dayton, Civil, and Environmental Engineering.

Prof. Hui Wang

Contact Info.: *hcastaneda@tamu.edu*, phone: 9794589844

Table of Contents

Section A: Business and Activities

(a) Contract Activities

- Contract Modifications:

  No contract modifications have been considered or executed during this first year.

- Educational Activities:

  - Student mentoring:

  We organize weekly meetings in the corrosion group for research updates and activities performed. Each student is assigned a senior researcher to follow up on the activities and discuss the results obtained. The students participate in the laboratory activities.

  Monthly meetings are scheduled to follow up on the student's activities and discuss the results with the technical team.

  - Student internship:

  No student internships have been planned or taken during the first year.

  - Educational activities:

  The experimental setup has been used for different training activities. Mr. Tristan De Servis offered reflectometry training in August. Graduate and undergraduate students were able to take the course. The course took four days and covered all the technology aspects and hands-on practice. Task 1 involved the use of this technology to perform different experiments.

  - Career employed:

    Nothing to report

- Dissemination of Project Outcomes:

  We submitted two abstracts to the AMPP 2025 annual conference and they were accepted. We are preparing two abstracts for the Orlando conference.

- Citations of The Publications:

  No publications are reported for this year.

(b) Financial Summary

- Federal Cost Activities:

- PI/Co-PIs/students involvement (including total):

  Total: $33,740.29

- Materials purchased/travel/contractual (consultants/subcontractors):

  Total is: $40,546.05

  Total Direct costs: $74,286.34

  Total: $104,989.32

- Cost Share Activities:

  - Cost share contribution:

- Heuristech has contributed $22,400 in technology training and/or company personnel hours for physical laboratory testing and mathematical tools.
- Integrity Solutions has contributed $6,500 in CP field data collection, technical staff resources to collect, collate, evaluate, screening, database development, attending workshops and training, analyzing Cathodic Protection (CP) data, contributing to computer algorithm development programming, and other program software/model components.
- The University of Dayton has contributed $24,348.89 in cost share, $16,178.66 in faculty payroll and $8,170.23 in indirect costs.

(c) Project Schedule Update

- Project Schedule:

Table 1. Timeline and schedule for the project in Gantt chart.

Task/Subtask	Fiscal Year											
	2023	2024				2025			2025	2026	2026	2(
	Q4	Q1	Q2	Q3	Q4	Q1	Q2	Q3	Q4	Q1	Q2	(
Task 1: Designing and building the physical prototypes in laboratory conditions and deterministic modeling												
Task 2: Integrating field inspection, theoretical with experimental data by applying pattern recognition techniques relating the pipeline-coating-soil system with CP												
Task 3: Validation of the *a priori* framework with experimental and field conditions for characterization/modeling and Evaluate/Validate												
Task 4: Development and validation of the methodology for ECDA based on CP levels												

Deliverable Milestones are indicated in black*

- Corrective Actions:

We have been working in the theoretical and laboratory very actively during the last quarter and we will increase the number of people working in the laboratory for the experimental setup and experimental testing. We have one PhD graduate in the summer and we are training another couple of PhD students. Task 1 needs to be completed on time and successfully, the action is more the mentoring and recruiting.

Task Risk	Priority	Risk Description	Impact Summary	Response Strategy
Experimental setup and design-Task 1	High	-Build samples to represent the conditions of far-distance steel Pipelines	The samples to be used in the laboratory are critical for understanding and simulating the far-location pipeline conditions.	Risk Avoidance Training and selecting the most critical parameters to finalize the experimental matriz

Section B: Detailed Technical Results in the Report Period

1. Background and Objectives in the 2nd Annual Report Period

Background

Carefully designed laboratory studies will be conducted to evaluate different electrochemical properties for detecting and characterizing defects in the coatings and active corrosion at the coating/substrate interface under cathodic protection conditions. These studies will define and analyze the EIS, potential profile, and reflectometry data under different pipeline/coating /electrolyte and CP configurations. The experimental variables in Figure 2 will include different coating anomalies, types of coating, and soil properties (such as resistivity, pH, humidity, ionic content), under different CP conditions. In particular, we will explore the characterization and assessment of the polarization in coatings/steel interface and corrosion severity. This task includes designing and constructing the physical model simulating field conditions. Figure 3 illustrates an example of the physical design of the pipeline under CP conditions and the soil environment.

This task aims to experimentally characterize the potential profile in different environments at the laboratory scale. The testing results will extract the most sensitive parameters/indicators for a comprehensive performance based on different levels of CP (based on the -850-mV vs. $Cu/CuSO_4$ criterion). Different coating conditions (intact and damaged) in steel/soil system samples under CP-simulating operation conditions will generate valuable information for assessment and validation. Experimental methods proposed in previous works by using EIS [3,14], reflectometry [11], and potential profile [12] will help to generate three critical outputs. The first level of experimental parameters will include coating anomalies and different soil conditions. The standard Practice 0169 (NACE SP 0169) CP level will reference several DC polarization conditions (from -600-mV to -1500 vs. $Cu/CuSO_4$). These experimental variables can be correlated with the mechanisms occurring at the steel–coating interface.

Objectives in the Annual Report Period

The herein proposal includes the following objectives:

- Develop a unique experimental-mathematical modeling platform with data-driven modeling that will serve as an external corrosion assessment tool for the identification and quantification of CP effectiveness.
- Integration of classic indirect techniques and direct new technology via reflectometry to assess the CP.
- Quantification of risk and repairing action is considered based on the outcome of the methodology developed.

2. Theoretical Program in the Annual Report Period

Theoretical Deterministic Model

To develop the governing equations three main assumptions of the system were made:

1. The top and bottom channel impedances ere assumed to be homogenous over the entire domain

2. Top channel consisted of only resistive elements to simulate the resistance of the surrounding environment and the impedance of the bottom channel of the TLM was negligible due to the highly conductive nature of the metallic substrate.

3. Interfacial impedance was assumed to be homogenous over the region for which it was defined. To simulate heterogenous interfaces, the interfacial impedance was defined for each region and the resulting governing equations were solved piecewise.

Applying the above assumptions, a system of equations can be developed for initial implementation of the 2D TLM for both homogeneous and heterogeneous cases. Figure 1a,c shows a representation of the homogenous and heterogenous systems used for the developing the governing equations of the 2D TLM. The cross sections in Figure 1b,d show the distribution of interface impedances, the transverse impedance for the coating and holiday regions are represented by Z_c and Z_h respectively. A unit cell for a generalized 2D TLM system is shown in Figure 1e.

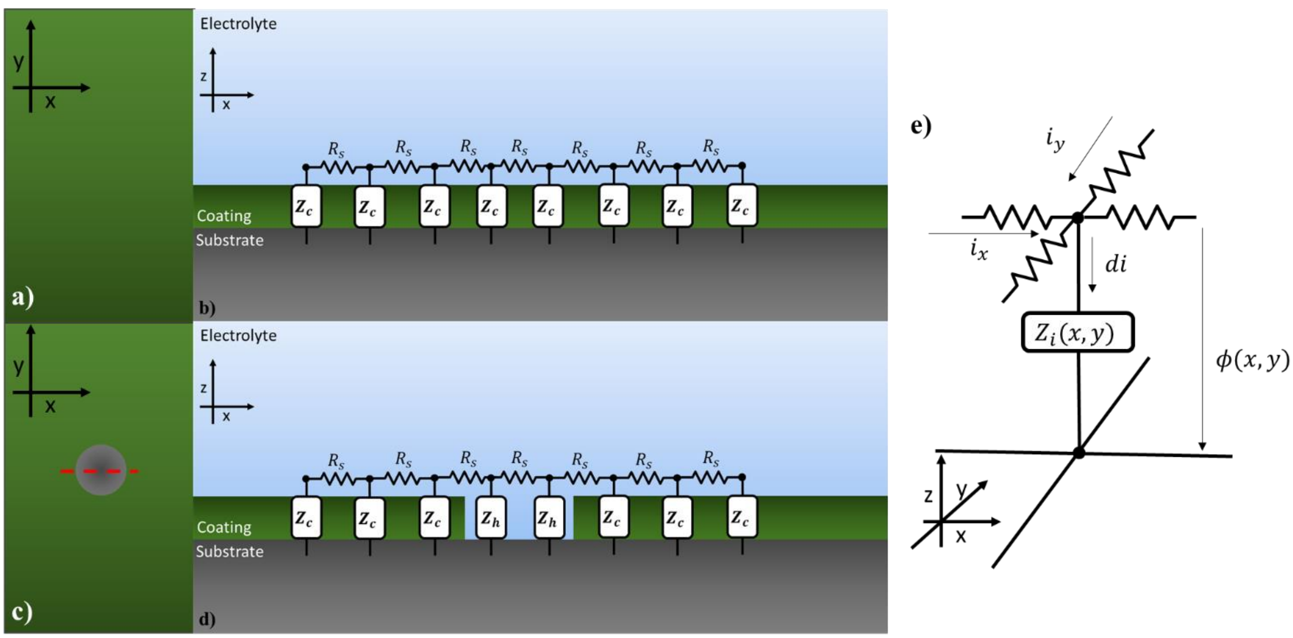

Figure 1: a) Homogenous coating, b) cross section showing the impedance distribution inside the coating, and c) heterogenous surface, and d) cross section of the coating with a holiday to display the changes in transverse impedance from the coating to inside the holiday, and e) 2D TLM unit cell system

Since the process for deriving the governing equations is the same for homogenous and heterogenous case. The process is only described for the heterogenous case. Governing equations are then be constructed for each of their respective regions and solved piecewise numerically. Coating and holiday regions are labeled as region 1 ($\mathbb{R}_1$) and region 2 ($\mathbb{R}_2$) respectively.

Potential and current distributions for the heterogenous case along with the resulting potential PDEs are shown in equations 1-5.

$$-\phi = (\nabla \cdot \vec{\imath}) Z_c \quad (x, y) \in \mathbb{R}_1 \tag{1}$$

$$-\phi = (\nabla \cdot \vec{\imath}) Z_h \quad (x, y) \in \mathbb{R}_2 \tag{2}$$

$$\vec{\imath} = -\frac{1}{R_s} \nabla \phi \tag{3}$$

$$-\left(\nabla \cdot \left(-\frac{1}{R_s} \nabla \phi\right)\right) - \frac{1}{Z_c} \phi = 0 \quad (x, y) \in \mathbb{R}_1 \tag{4}$$

$$-\left(\nabla \cdot \left(-\frac{1}{R_s} \nabla \phi\right)\right) - \frac{1}{Z_h} \phi = 0 \; (x, y) \in \mathbb{R}_2 \tag{5}$$

The PDEs were solved using finite element method (FEM) PDE solver that was pre-built into MATLAB software. After the calculation of the potential and current distribution the local impedances were then calculated.

$$z_k = -\frac{\phi_k}{(\nabla \cdot \vec{\imath})_k} \tag{6}$$

Where the z_k is the transverse impedance, ϕ_k is the local potential, and $(\nabla \cdot \vec{\imath})_k$ is the divergence of the current evaluated at k^{th} node. The global impedance is then calculated from the local impedances following the approach of Huang et al. [1] that was based on the treatment of the distribution of admittance by Brug et al. [2].

$$Z = \left\langle \frac{1}{z_k} \right\rangle^{-1} \tag{7}$$

For validation of the 2D TLM model the modeled impedance will be fit to experimental data, where specific EEC values will be determined to provide the best fit as possible. The fitting of complex data is best performed by fitting the real and imaginary parts of the impedance simultaneously [3]. For performing the best fit of the EEC values a complex non-linear least square fitting (CNLLSF) can be used. Marquardt developed an initial algorithm for CNLLSF in 1963 [4], and has led to several CNLLSF methods and algorithms to be develop for fitting impedance/admittance data [3, 5-8]. Following the procedure laid out by Boukamp [6], a CNLLSF function was written to perform the fitting of EEC values used in the 2D TLM model to experimental data to find the best fit between the model and experimental data.

For initial numerical analysis of the 2D TLM, the interfacial impedance was assumed to be modeled as a one-time constant EEC with resistance and CPE element in parallel that is applicable for modeling numerous simple electrochemical systems. Figure 2 shows the sensitivity analysis of EEC used as the transverse impedance of the homogenous system. Figure 2 (a-c) show the effect of the CPE parameter (n1) on the global impedance. It can be seen that with decreasing n value the maximum point of the semi-circle loop becomes depressed and the phase angle shifts to more positive values. Showing that the CPE changes from ideal capacitive behavior to more a more resistive one. From Figure 2 (d-f) with decreasing Q1 values while keeping other circuit value constants shows a shift in the frequency response of the circuit to higher frequencies. Showing that if there is a shift in the capacitive values while others are held constant there is only shift in the frequency response of the system, and not in the overall impedance magnitude. The effect of changing R1 can be seen in Figure 2 (g-i), where with decreasing R1 the total impedance decreased. Overall, the sensitivity analysis of the homogenous case behaved very similar to that of a lumped EEC. Due to the assumption that only EEC was used to describe the impedance of the interface.

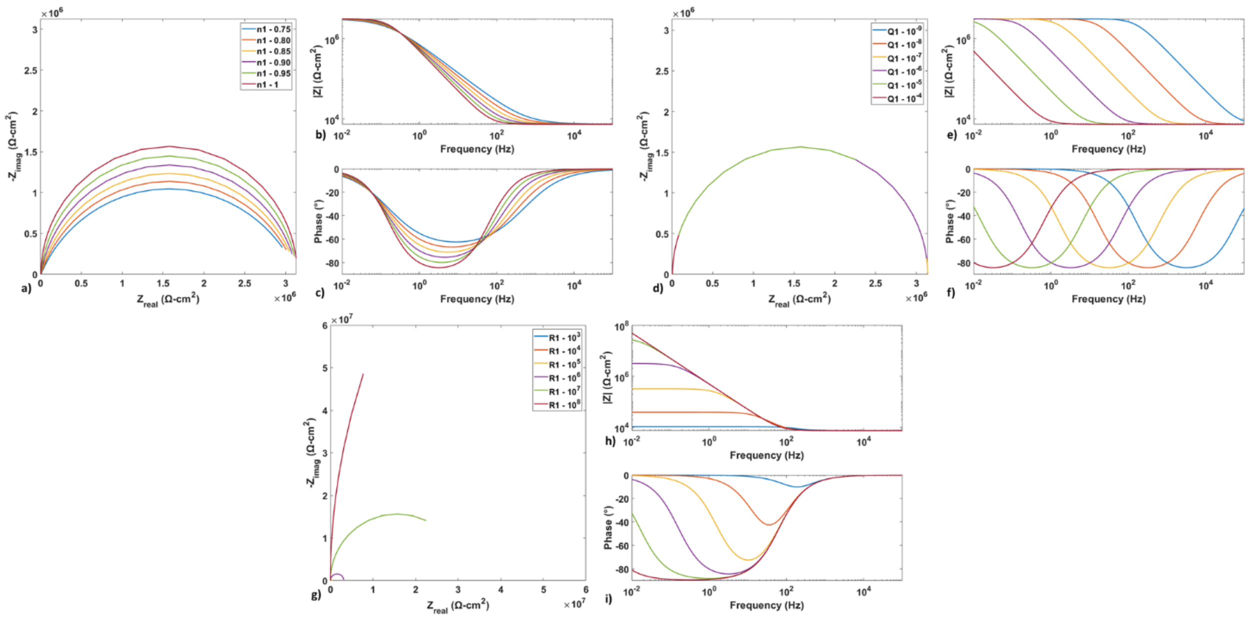

Figure 2: Homogenous System sensitivity Analysis of EEC-2 where base circuit values were set to R1 = 1e6 Ω, Q1 = 1e-6 F-s^{-n}, and n1 = 1, (a-c) Effect of changing n1 on the Nyquist, Bode, and phase angle plots, (d-f) Effect of changing Q1 on the Nyquist, Bode, and phase angle plots, and (g-i) Effect of changing R1 on the Nyquist, Bode, and phase angle plots

For studying the sensitivity of the model in the heterogenous case, the geometry of the heterogenous system is shown in Figure 3. Where the dimension of $\mathbb{R}_1$: diameter = 2 cm, area = 3.122 cm^2 and dimensions of $\mathbb{R}_2$: major axis = 0.15 cm, minor axis = 0.05cm, and area = 0.0236 cm^2. Initially it was chosen for the area of $\mathbb{R}_2$ to be several orders of magnitude lower than the total area to understand the effect of small areas of local impedance changes on the total impedance of the system.

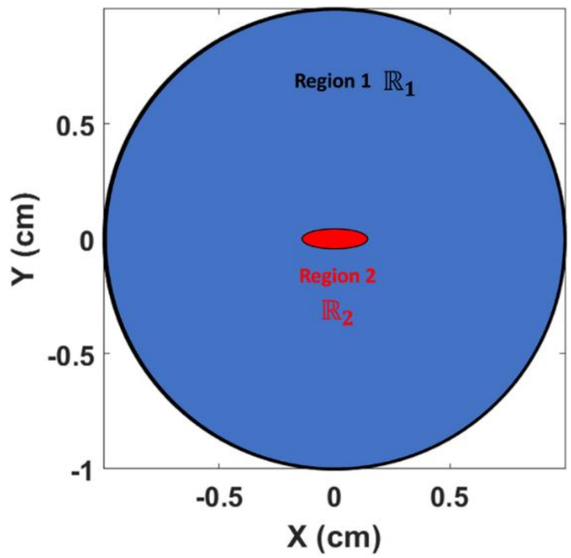

Figure 3: Geometry of heterogenous systems used for sensitivity analysis

For both regions same single time constant EEC was chosen as the model's transverse impedance. Allowing for considerable customization of the electrochemical system that the model can be applied to. The EEC parameters for $\mathbb{R}_1$ were set to: R1 = 1e8 Ω, Q1 = 1e-8 F-s^{-n}, and n1 = 1 these values were chosen to represent passive/protected interface. Figure 4 shows the sensitivity analysis for the heterogenous system for the varied EEC circuit parameters of $\mathbb{R}_2$. The black curve Figure 4 represents the homogeneous case using the same circuit parameters as those used for $\mathbb{R}_1$.

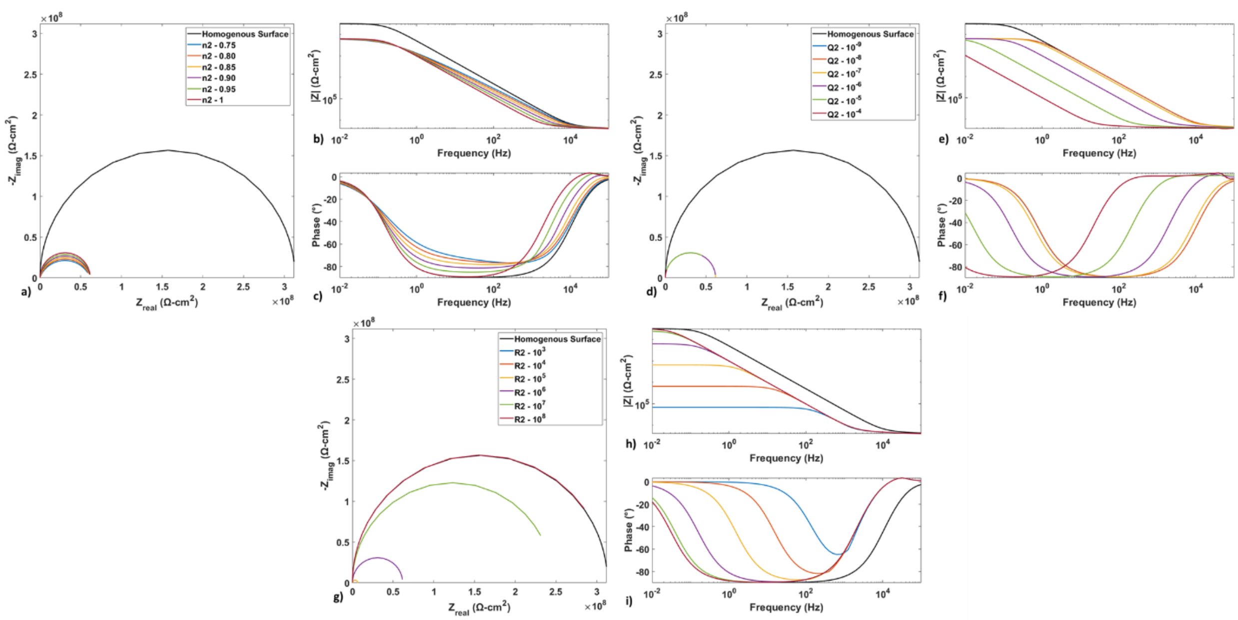

Figure 4: Heterogenous System sensitivity analysis of changing values associated with $\mathbb{R}_2$, base circuit values were set to: R2 = 1e6 Ω, Q2 = 1e-6 F-s^{-n}, and n2 = 0.85, (a-c) Effect of changing n2 on the Nyquist, Bode, and phase angle plots, (d-f) Effect of changing Q2 on the Nyquist, Bode, and phase angle plots, and (g-i) Effect of changing R2 on the Nyquist, Bode, and phase angle plots

Comparing the homogenous case (black curve) to the various heterogenous cases in Figure 4(a-f), it can be seen that the overall impedance is heavily affected by the low impedance area. Even with almost two orders of magnitude of difference in surface area the introduction of the are of low impedance lowered the global impedance by almost a full order of magnitude. Generally, the sensitivity of the system to changing circuit parameters behaved the same as the homogenous case. Where the effect of changing CPE parameters (Q2 and n2) shown in Figure 4(a-f) showed that with decreasing n values the Nyquist plots showed a depression of the semi-circle, and a shift to more positive phase angle values and changing Q values affect the frequency response of the system. From Figure 4 (g-i) it can be seen the R2 values played a large part in the overall impedance, and with increasing resistance values the overall impedance increased to values near the homogenous case. The impedance response does not exactly match the homogenous cause due to the CPE parameters in $\mathbb{R}_2$ being different than in $\mathbb{R}_1$. Figure 5 shows the effect of changing R2 values of $\mathbb{R}_2$ from 1e2 – 1e12 Ω while keeping the CPE values constant. This was done to show the effect changing the impedance of $\mathbb{R}_2$ to values equal and or higher in magnitude compared to $\mathbb{R}_1$.

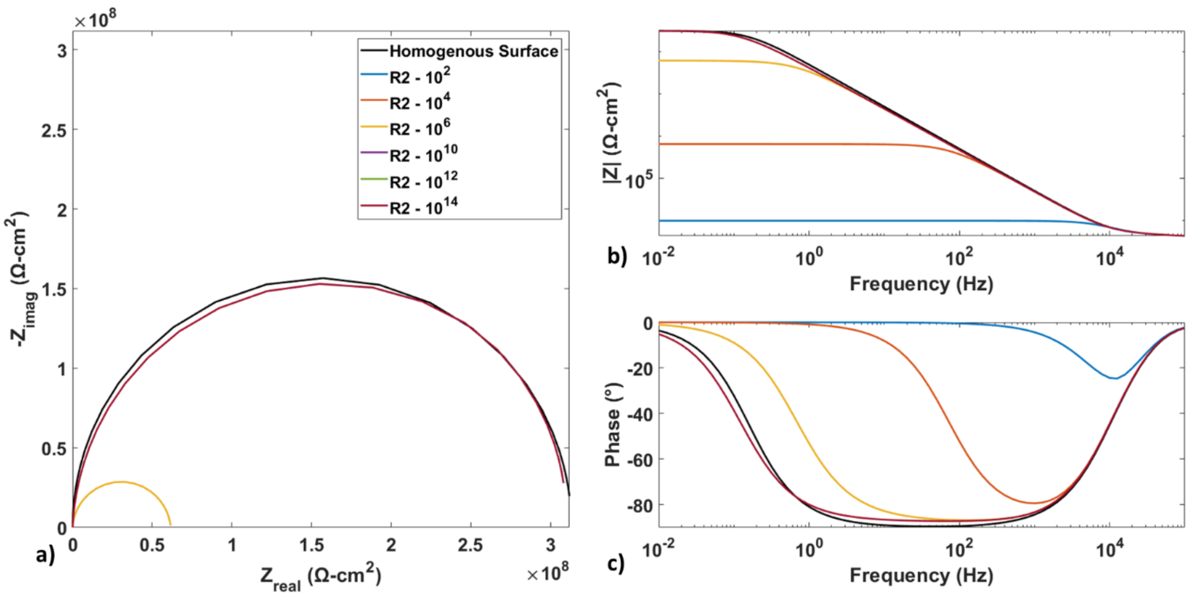

Figure 5: Heterogenous System sensitivity analysis of changing values associated with $\mathbb{R}_2$, base circuit values were set to Q2 = 1e-6 F-s^{-n}, and n2 = 0.85, Effect of changing R2 on the a) Nyquist, b) Bode, and c) phase angle plots

From Figure 5 it can be seen that when the resistance in $\mathbb{R}_2$ is less than that of the surrounding area the global impedance of the system is lower than the homogenous case. But, when the resistance of $\mathbb{R}_2$is higher than the surrounding area the global impedance of the heterogenous system is very close to that of the homogenous surface. Showing that the global impedance of the system is heavily dependent on the lowest impedance region of the system.

The 2D TLM can also calculate the local impedances distribution across the interface as well as the overall impedance using equations 24 and 25 respectively. Using the model geometry shown in Figure 3, a heterogenous model was created with two regions of varying impedance to see the local distribution of impedance in a heterogeneous system. Model input parameters for the two regions are shown in Table 1. The impedance of the heterogenous system was compared to two homogenous systems, where one was using high impedance EEC values and the other the low impedance EEC values. Figure 6 shows the comparison of the global impedance response of the heterogenous system with the two homogenous systems.

Table 1: EEC values of the two regions of the heterogenous system

	High Impedance region ($\mathbb{R}_1$)	**Low Impedance region ($\mathbb{R}_2$)**
R (Ω)	**1E8**	**1E4**
Q (F-s^{-n})	**1E-8**	**1E-4**
n	**1.00**	**0.85**
R_s (Ω)	**500**	**500**

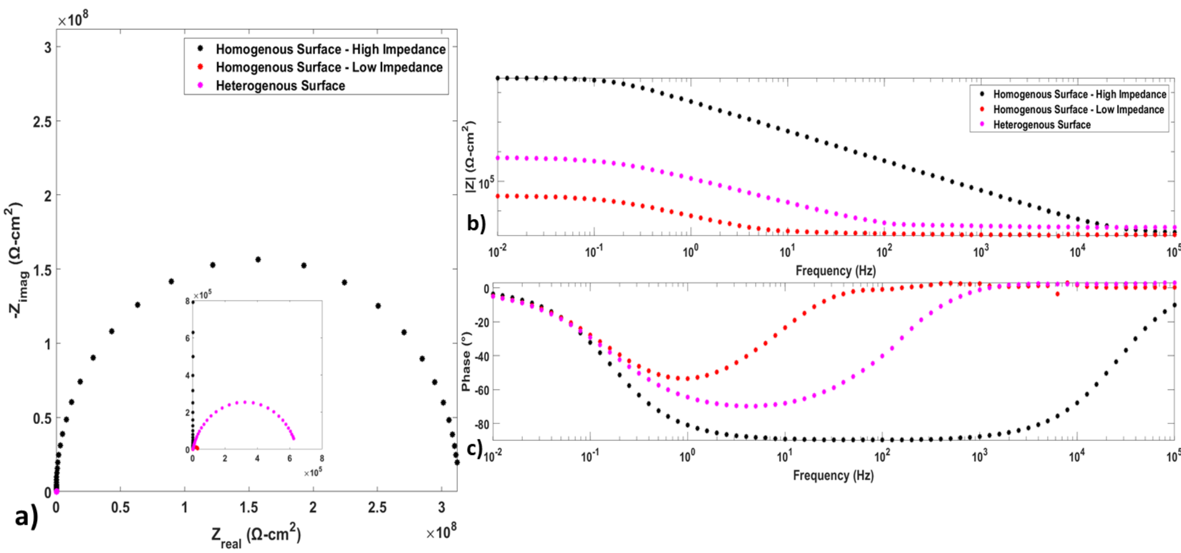

Figure 6: (a) Nyquist, (b) Bode, and (c) Phase angle plots comparing the overall impedance of the heterogenous surface consisting of both high and low impedance (magenta curve) compared to high (black curve) and low (red curve) homogenous surfaces.

From Figure 6b it can be seen from the bode plots that the magnitude of the all three systems start near the same value (R_s) and increase to their respective low frequency magnitudes. The impedance response of the hetergenous systems falls in between that of the low and high impedance homogenous systems. This shows that the global impedance of the heterogensou model takes into account all of the impedances of the system, but the global impedance of the heterogenous system is more weighted more towards the lowest impedance of the sytem. To further understand how the overall impedance response varies from the homogenous cases, the local distrubtions of impedance magnitude (|Z|) and phase angle for the three systems at 10 Hz are shown in Figure 7. Comparison of the average values of |Z| and phase angle for the three systems are in Table 2.

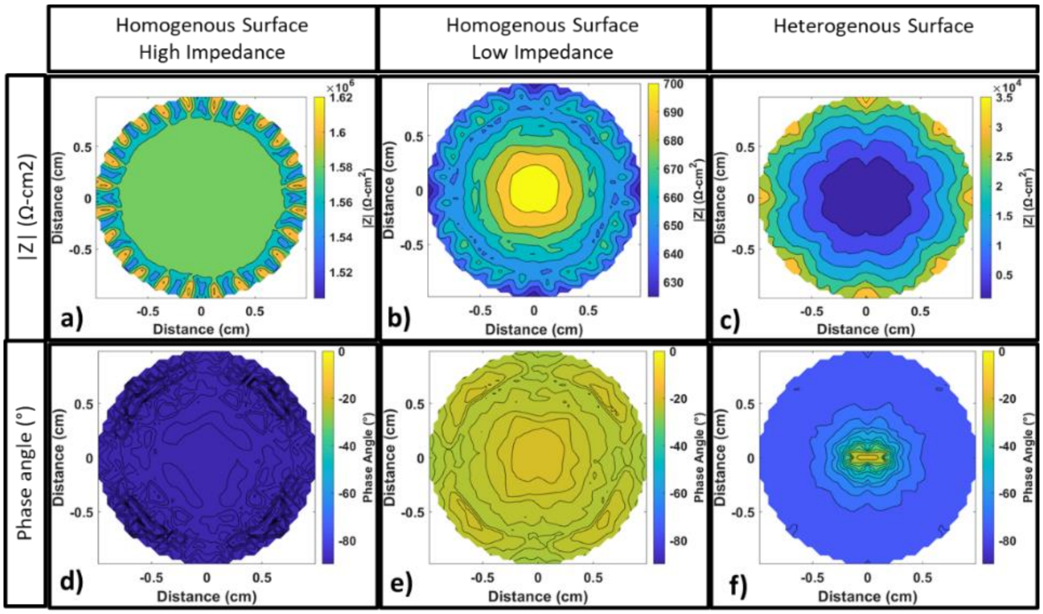

Figure 7: |Z| and phase angle distribution at 10 Hz for (a,d) high impedance homogenous system, (b,e) low impedance homogenous system, and (c,f) heterogenous system.

Table 2: Comparison of the average |Z| and phase angle values for three modeled systems at 10Hz

	Homogenous System High Impedance	**Homogenous System Low Impedance**	**Heterogenous System**
|Z| (Ω-cm^2)	$\mathbf{1.58E6 \pm 1.55E4}$	$\mathbf{664.66 \pm 17.88}$	$\mathbf{1.57E4 \pm 8.96E3}$
Phase Angle (°)	$\mathbf{-89.04 \pm 8.56 - 4}$	$\mathbf{-23.45 \pm 1.38}$	$\mathbf{-69.78 \pm 9.10}$

As was to be expected for the homogenous cases there was relatively little variation of the |Z| and phase angle values across the surface, while the heterogenous case showed a larger variation due to the different regions. The |Z| magnitude of the heterogenous cause ranged from around 3.25E4 Ω near the boundaries far away from the low impedance region and decreased to values around 1000 Ω near the center of low impedance region. From the contour map in Figure 7c shows that the |Z| of the heterogenous system gradually decreases in value from the boundary to the system. For the three systems the average phase angle shifted to more positive values with the homogenous high impedance system at -89°, heterogenous system at around -70°, and the homogenous low impedance value at the most positive around -23°. From Figure 7(d-f) the phase angle of the homogenous systems did not vary much spatially, but for the heterogenous case there was relatively steep increase as you get closer to the low impedance area boundary. Inside the low impedance region, the phase angle was relatively constant around -20° which is close to the average value of the homogenous low impedance surface.

3. Experimental Program in the Annual Report Period

Experimental Design

The experimental test matrix is shown in Table 3. Base metal and coating were chosen specifically selected to try and simulate the most commonly used materials in the field. Currently all lab testing is being performed with 1018 CS base metal and fusion bonded epoxy (FBE) coating that is applied in house. With plans to include the other base metals and commercially applied coatings. The testing solution for all testing was selected to be NS4 solution with various pH values. This solution simulates the near soil environment seen in the field and consists of 4 chemicals: sodium bicarbonate ($NaHCO_3$), potassium chloride (KCl), Calcium Chloride ($CaCl_2$), and magnesium sulfate heptahydrate ($MgSO_4$-$7H_2O$). Exact composition and methods for altering pH are detailed below. The cathodic protection (CP) and coating state were varied to simulate the various conditions that in use pipelines can be found. Understanding how the CP level and coating state affect the impedance response of the system can provide more insight into detecting problems with pipelines earlier and with more accuracy.

Table 3: Experimental Test Matrix

Base Metal	Testing Solution	CP State (mV vs SCE)	Coating	Coating State	Coating Thickness (mil)
1010/1018	NS4 – As-recived	OCP (no protection)	Coal Tar	Intact	15
X52	NS4 – Neutral pH	-637 (under protection)	FBE	Holiday – small	20
X68	NS4 – Acidic pH	-777 (standard protection)	Yellow Jacket	Holiday – large	25
		-1227 (over protection)	Tri-layer	Delamination	35
					45

Test Procedure

- <u>Laboratory Testing</u>

1018 carbon steel plates were coated with a commercial grade FBE. The thickness of the coating was varied from 10 mil to 50 mil. Coating thickness was controlled with a micrometer adjustable film applicator. sdTwo initial studies were performed with the FBE coatings: 1) effect of coating thickness on impedance response of the system with and without holidays at OCP, and 2) Effect of CP state for a coating with a thickness of 25 mil under the three-coating states (intact, holiday, and delamination). For the initial holiday creation, the holiday was of square geometry and was cut by hand into the coating after the coating was fully cured. The dimensions of the holiday were 0.5 cm x 0.5 cm (0.20” x 0.20”) giving a surface area of 0.25 cm^2 (0.039 in^2). Going forward all holidays were created with a circular geometry and were cut with an endmill to insure that the created holidays are consistent. The diameters of the small and large holidays are 0.516 cm (0.203”) and 0.794 cm (0.313”) respectively. To simulate the delamination’s in the lab small domes of FBE were created and then attached to the surface. Figure 8 depicts the delamination geometry.

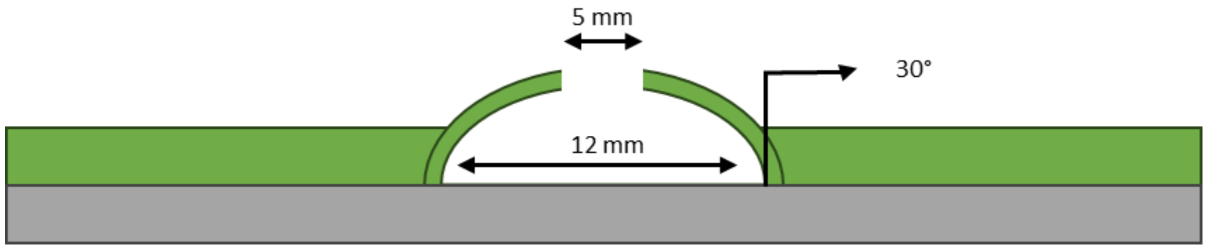

Figure 8: Delamination geometry

NS4 solution was used as the testing solution to simulate the corrosion of buried pipelines. NS4 is a soil mimicking solution that consists of potassium chloride (0.122 g/L), sodium bicarbonate (0.483 g/L), calcium chloride (0.137 g/L), and magnesium sulfate heptahydrate (0.131 g/L). To adjust the pH of the solution various concentrations of CO_2/N_2 were purged through the solution, where increasing the amount of bicarbonate in the solution lowers the pH of the solution [9].

All electrochemical testing was performed at ambient conditions with a three-electrode system. Where a saturated calomel electrode (SCE) was used as the reference electrode, platinum mesh as the counter electrode, and the tested material as the working electrode. EIS measurements were performed by applying a sinusoidal perturbation while varying frequencies from 100 kHz to 10 mHz. For the intact coating samples the potential perturbation was set to 15 mV_{rms} and for samples with defective coatings it was set to 10 $mV_{rms.}$ A large potential signal was applied to the intact coating samples to increase the current response of the system lowering the amount of the noise in the measurements. To simulate the various levels of CP the DC bias potential for the EIS signal was set to the specified potentials.

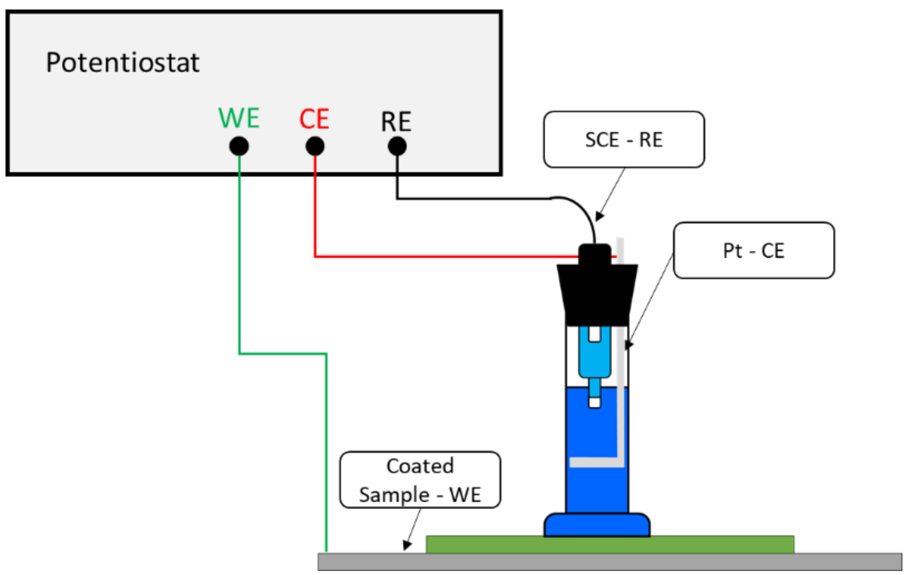

Figure 9: EIS testing schematic

After performing OCP, LPR, and EIS, the samples underwent decay testing. Starting with the OCP measurement, the initial potential was selected in the anodic direction of the process at +0.1V from the OCP. The schematic test system was set up as shown in Figure 2. The power supply was connected to apply the selected potential condition. The system was held for 30 seconds to ensure stability, after which the power supply was turned off, and the potential was measured using a voltmeter for 600 seconds to confirm that stability remained.

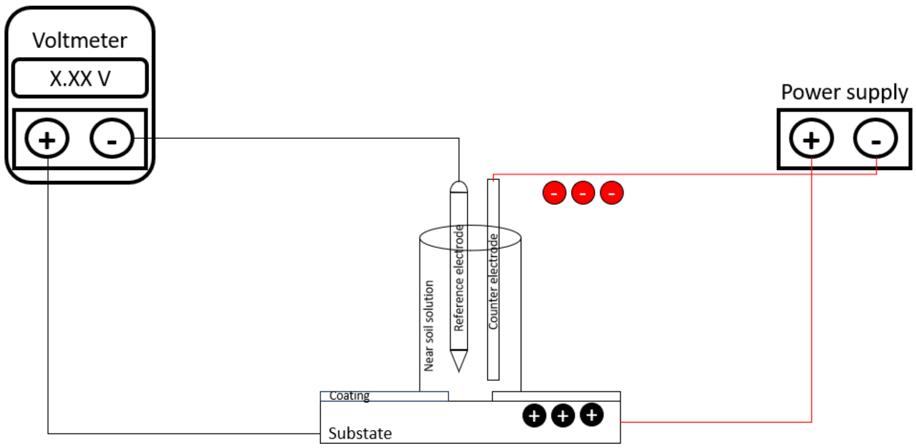

Figure 10: Schematic illustration for the anodic decay setup of the tests

- <u>Field Testing:</u>

4. Results and Discussions

Task 1: Designing and building the physical prototypes in laboratory conditions and deterministic modeling

- <u>Task 1.1: Electrochemical Impedance Spectroscopy Study</u>

This is initial set of data was performed with the square holiday geometry as a proof of concept. Figure 11 shows the Nyquist, Bode, and phase angle plots of FBE coated carbon steel after 1-week immersion and the fitted 2D TLM. The coated samples displayed phase angle values near -90° which shows that the coating behaving like a perfect capacitor and still protecting the base material. The EEC values determined from CNLLS fitting are shown in Table 4. The fitted values of the EEC were able to fit the experimental data relatively well, showing the viability of the model for use with high impedance systems. In the low frequency regime, it can be seen that the phase angle starts to bend towards more positive values. This shift in phase angle values is most likely due to water uptake into the coating. Which displays the ability of the model to still perform well when the impedance of the electrodes tends towards non-ideal behavior.

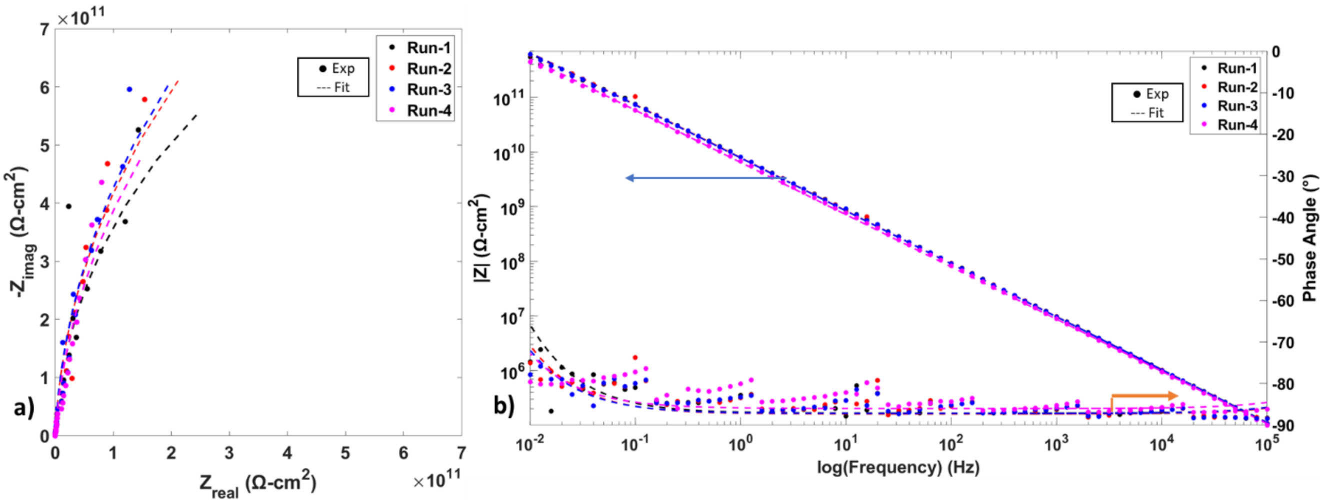

Figure 11: a) Nyquist and b) Bode and phase angle plots of coated carbon steel in NS4 solution after 1 week immersion

Table 4: CNLLS Fitted values of EEC values used in 2D TLM for coated carbon steel in NS4 solution

Sample	*R (Ω-cm²)*	*Q (F-cm²-s⁻ⁿ)*	*n*	*RMS Error*
Run 1	$1.69 * 10^{12} \pm 1.37 * 10^{11}$	$2.17 * 10^{-11} \pm 2.74 * 10^{-13}$	0.968 ± 0.0015	0.0716
Run 2	$2.29 * 10^{12} \pm 2.92 * 10^{11}$	$2.14 * 10^{-11} \pm 2.55 * 10^{-13}$	0.970 ± 0.0014	0.0682
Run 3	$2.44 * 10^{12} \pm 2.95 * 10^{11}$	$2.17 * 10^{-11} \pm 2.17 * 10^{-13}$	0.969 ± 0.0012	0.0575
Run 4	$2.19 * 10^{12} \pm 3.84 * 10^{11}$	$2.68 * 10^{-11} \pm 3.41 * 10^{-13}$	0.956 ± 0.0015	0.0735

The EIS measurements of coated samples with a holiday introduced after one week immersion is shown in Figure 12. It can be seen that there is a drastic decrease in the overall impedance of the system compared to the impedance of the intact coating shown in Figure 11. In the model $\mathbb{R}_1$ was defined as the intact coating, an average value of the fitted EEC values from case 2 was used as the EEC values in $\mathbb{R}_1$. For the $\mathbb{R}_2$ the values were changed to provide the best fit possible. Initially the CNLLS function is not able to provide fitting for the heterogenous case, so fitting was performed manually, fitted EEC values are shown in Table 5. The model was able to provide the best fitting in the medium to low frequency ranges (< 10^1 Hz) and still had trouble with fitting in the high frequency regime most likely due to the system not taking into account systemic/random errors that can occur during measurements.

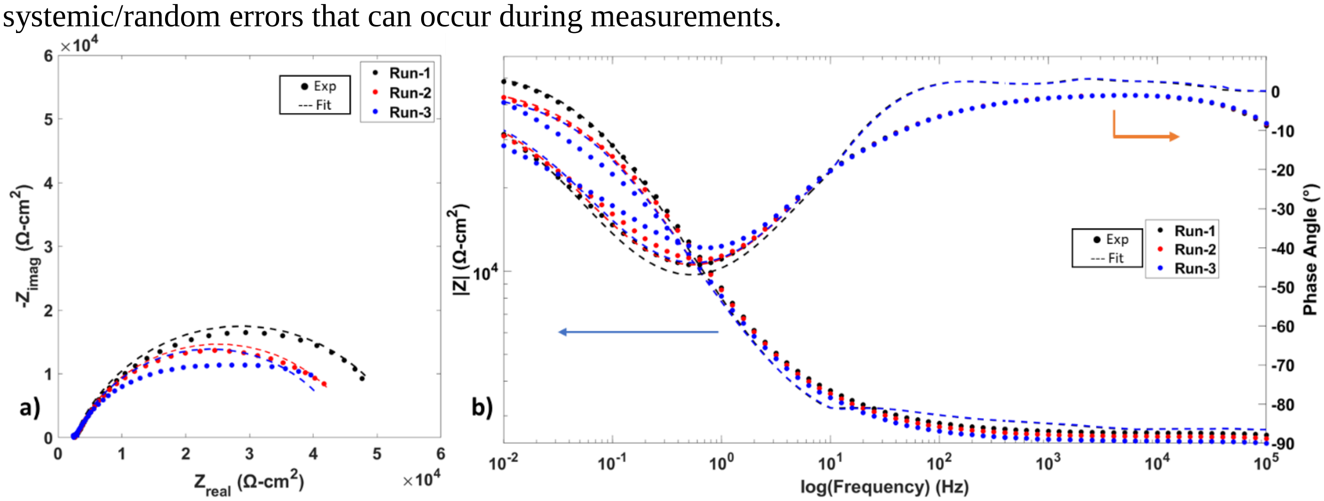

Figure 12: a) Nyquist and b) Bode and phase angle plots of coated carbon steel with coating holiday in NS4 solution after 1 week immersion

Table 5: Fitted values of EEC values used in 2D TLM for coated carbon steel with coating holiday in NS4 solution

Sample	*Region*	*R* *(Ω-cm²)*	*Q* *(F-cm²-s⁻ⁿ)*	*n*	*RMS Error*
Coating	$\mathbb{R}_1$	$6.86 * 10^{11}$	$7.19 * 10^{-11}$	0.966	-----
Run 1	$\mathbb{R}_2$	$1.73 * 10^{4}$	$1.10 * 10^{-3}$	0.750	0.1012
Run 2	$\mathbb{R}_2$	$1.49 * 10^{4}$	$1.18 * 10^{-3}$	0.733	0.1104
Run 3	$\mathbb{R}_2$	$1.41 * 10^{4}$	$1.18 * 10^{-3}$	0.733	0.1367

Traditionally a lumped EEC would be used for fitting the EIS data even when there are known heterogeneities in the system. Using the same EEC structure as was used in the 2D TLM, a lumped EEC was fit to the experimental data for comparison. The EEC values obtained by traditional lumped EEC circuit fitting is shown in Table 6.

Table 6: Lumped EEC fitting values

Sample	*R* *(Ω-cm²)*	*Q* *(F-cm²-s⁻ⁿ)*	*n*
Run 1	$3.84 * 10^{4}$	$3.58 * 10^{-4}$	0.700
Run 2	$4.56 * 10^{4}$	$3.70 * 10^{-4}$	0.691
Run 3	$4.33 * 10^{4}$	$4.28 * 10^{-4}$	0.654

Both the resistance and Q values of the lumped EEC values somewhere between the values used for the two regions shown in Table 5. This is most likely due to the lumped EEC taking an average of all the processes occurring with accounting for both the holiday and intact coating separately. The fitted resistance value is around two times higher in the lumped EEC compared to 2D TLM. This could lead to an under estimation of the extent of corrosion that is occurring at the holiday when calculating the local corrosion rate of the metal.

The |Z| and phase angle distributions at 10 Hz for the coating with square holiday is shown in Figure 13. The black lines on the indicate the model geometry. Outside the square assumed to be the intact coating ($\mathbb{R}_1$) and inside the square is assumed to be the holiday ($\mathbb{R}_2$). Both the |Z| and phase angle distributions display steady changes from the boundary of the model to just outside of $\mathbb{R}_2$, and then stays relatively constant inside of $\mathbb{R}_2$, and remained relatively constant inside of $\mathbb{R}_2$.

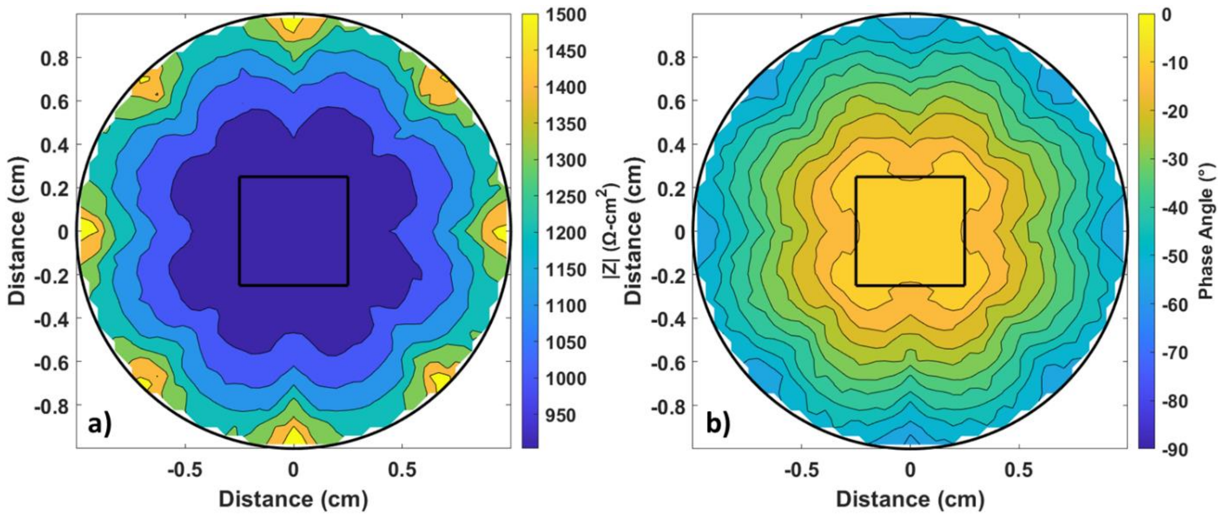

Figure 13: a) |Z| and b) phase angle distribution from 2D TLM at 10 Hz for coating with a holiday. Where the 2D TLM EEC values for the two regions are: $\mathbb{R}_1$ EEC values: $\boldsymbol{R = 2.18 * 10^{11}\ \Omega}$, $\boldsymbol{Q = 2.26 * 10^{-10}\ F - s^{-n}, n = 0.966}$ and $\mathbb{R}_2$ EEC values: $\boldsymbol{R = 1.57 * 10^{3}\ \Omega}$, $\boldsymbol{Q = 1.17 * 10^{-4}\ F - s^{-n}, n = 0.739}$

- <u>Task 1.2: Decay Study (Ken's Data)</u>

Figure 14 compares the potential decay of an intact coating and a coating with a holiday. It can be seen that for intact coating once the potential is turned off, the potential sharply changes once the applied signal is turned off and then holds steady at a plateau. For the coating with a holiday present the potential also sharply changes and then drastically decays exponentially.

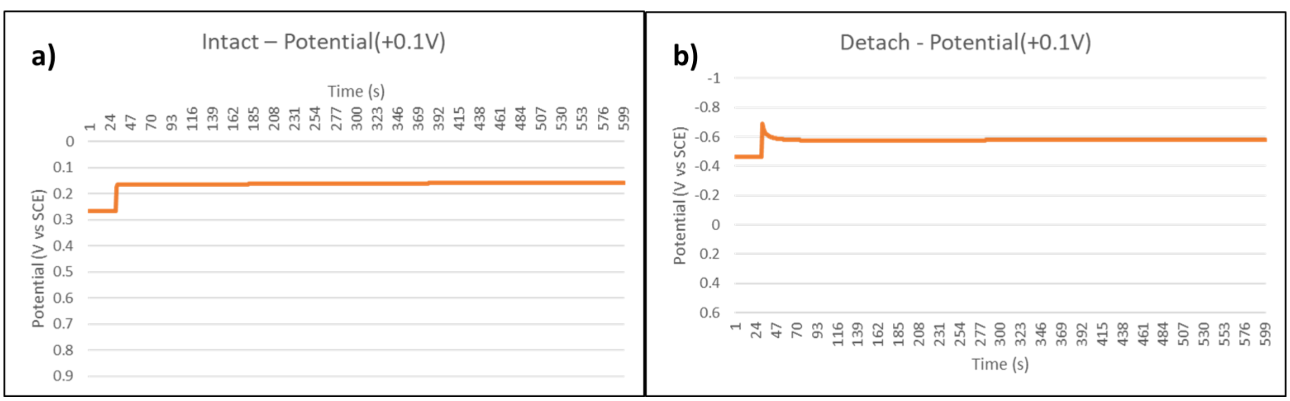

Figure 14: Comparison of the potential decay of a) intact coating, and b) coating with holiday

Figure 15 - Figure 17 show the effect of solution pH, holiday size, and applied potential on the potential decay of the system along with the EIS response of the system. For all three systems it shows that the systems displaying a higher overall impedance show a slower decay rate compared to the more active systems.

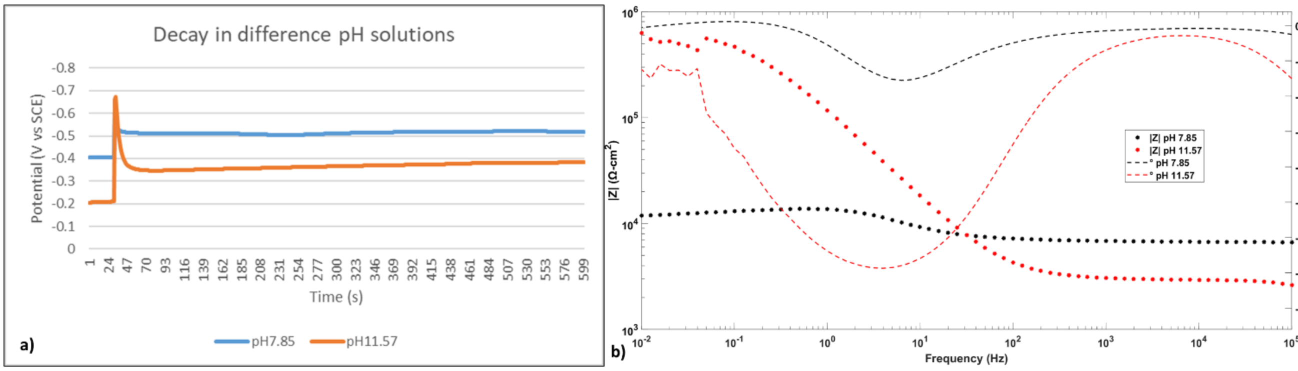

Figure 15: Effect of solution on pH on the a) potential decay and b) EIS response of FBE coating with holiday

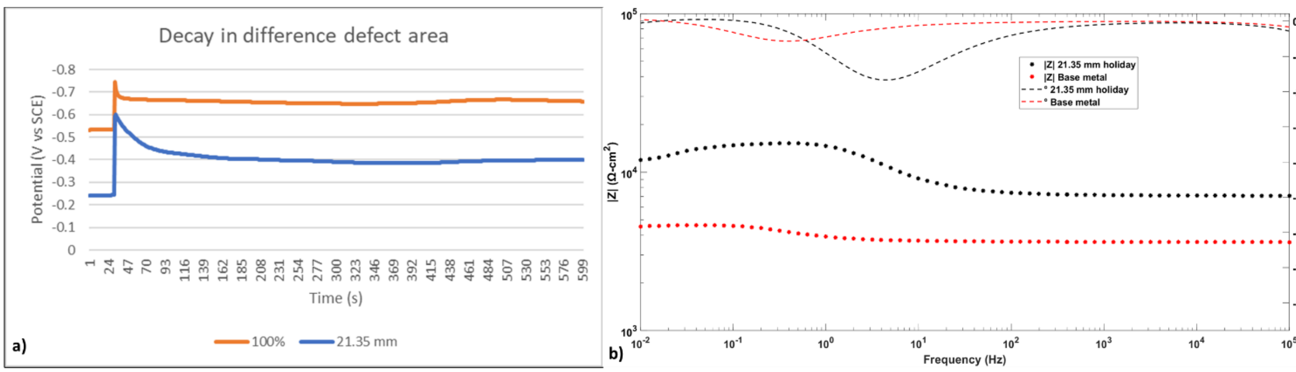

Figure 16: Effect of defect size on the a) potential decay and b) EIS response of FBE coating with holiday

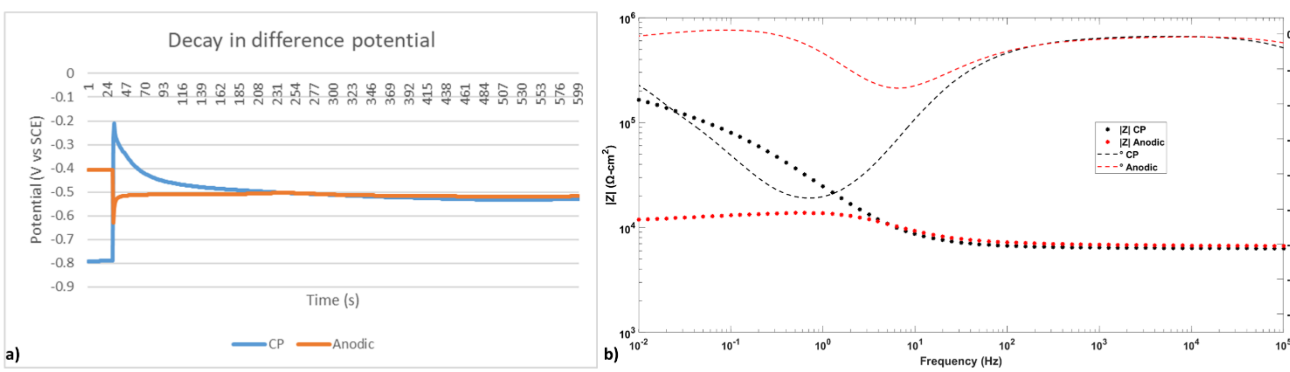

Figure 17: Effect of applied potential on the a) potential decay and b) EIS response of FBE coating with holiday

Task 2: Integrating field inspection, theoretical with experimental data by applying pattern recognition techniques relating the pipeline-coating-soil system with CP

Task 2.1: Data Integration (Field, Experimental and theoretical)

The focus of Task 2 is integrating field inspection, theoretical with experimental data by applying pattern recognition techniques relating the pipeline-coating-soil system with CP. In the past year, the University of Dayton team has conducted research work on field data collection, compilation, and fusion including both public data from open-source data repositories as well as private data from industry partners. More specifically, the private database contains asset information and historical inspection data of two pipeline system from industry sectors outside US. We are currently working with US based industry partners on data access and sharing and will have additional private pipeline data located in the US. Below we summarize the key investigations performed so far and major findings.

To effectively model the performance of Cathodic Protection (CP), based on our previous work mentioned in the project proposal, it is crucial to group pipeline sections with similar soil, climate, and environmental characteristics. To this end, the initial phase of the analysis involves creating a comprehensive digital database that captures the various features influencing corrosion and hence CP performance. These features are derived from a combination of remote sensing data and in-situ soil surveys. Figure 18 illustrates the satellite imagery obtained for the region of interest, along with the overlay of the pipeline right-of-way, while Figure 19 highlights key feature values gathered during the soil survey at the site. This integrated approach ensures that both large-scale environmental factors and localized soil conditions are accounted for in the corrosion modeling process, allowing for a more accurate assessment of CP effectiveness across different pipeline segments.

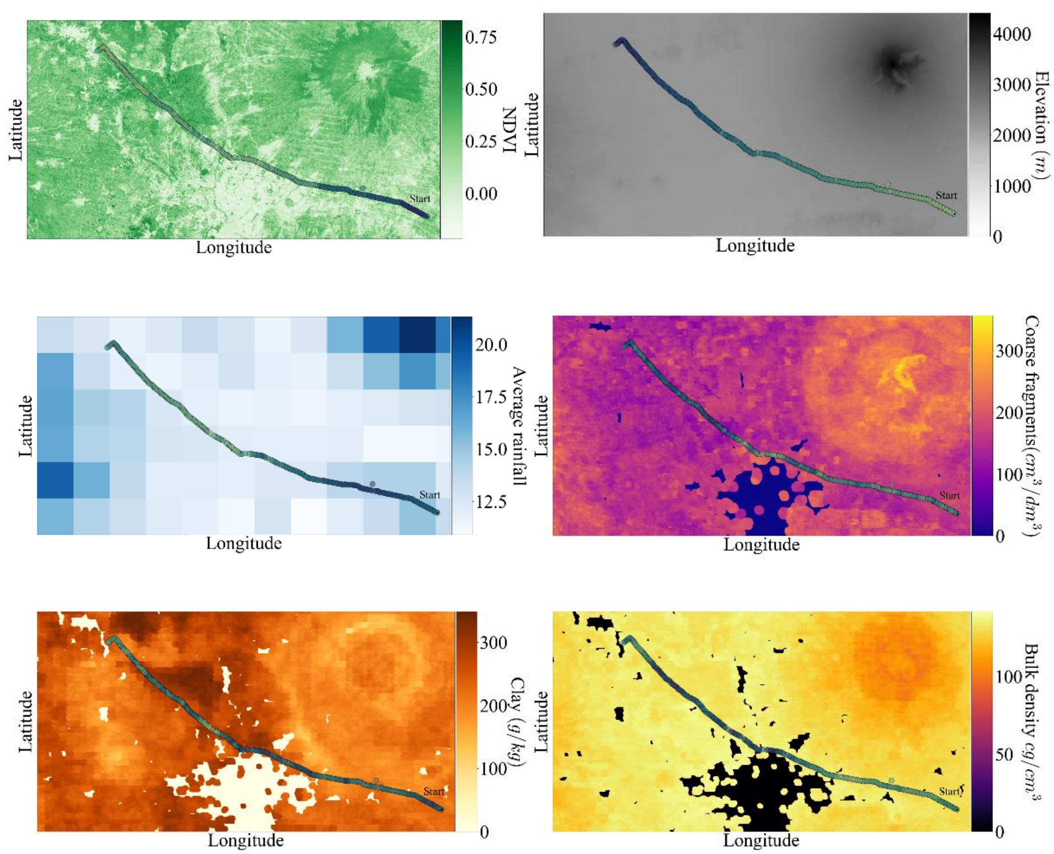

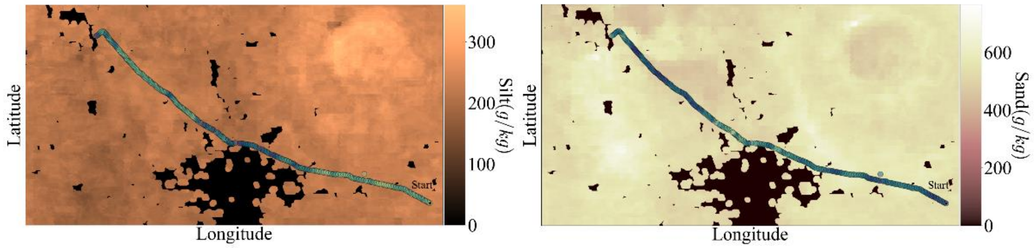

Figure 18: The map of features from satellite data within the region of interest and the overlay the pipeline right of way

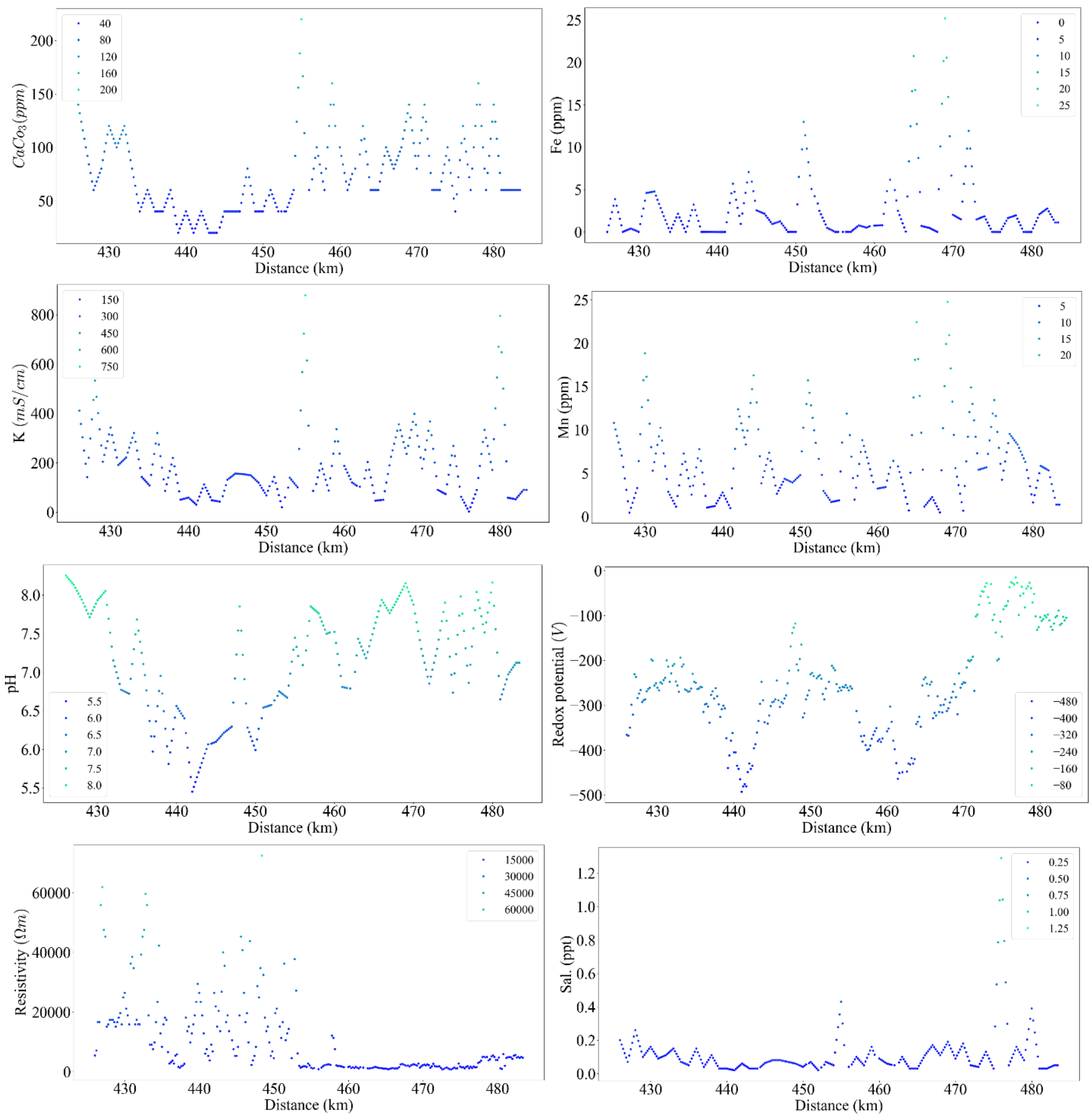

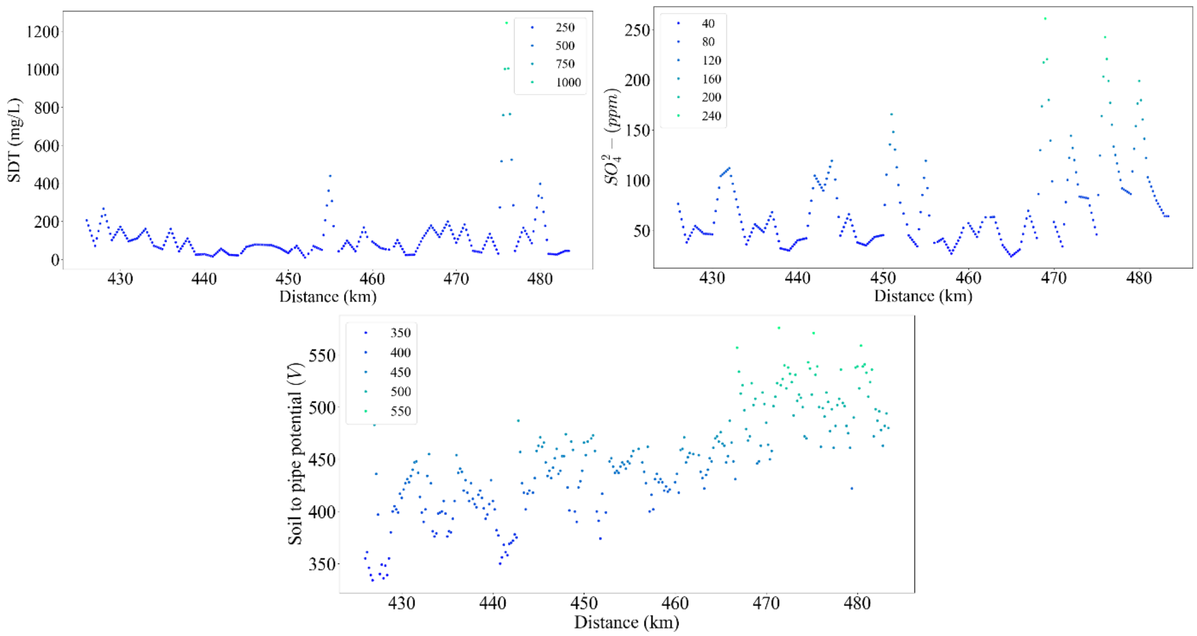

Figure 19: Soil survey data along the pipeline right of way.

Based on the collected and compiled data from remote sensing and soil surveys, from the perspective of data science, feature selection is conducted to identify the independent and informative variables that influence pipeline external corrosion. This process is essential for training and refining the model in downstream and improving its predictive accuracy while reducing redundancy and noise in the data.

Key Steps in the Feature Selection Process:

1. Data Preprocessing: The first step involves cleaning the data by handling missing values, removing outliers, and normalizing the features to ensure they are on the same scale. This ensures that no feature disproportionately affects the selection process due to differences in units or magnitude.
2. Correlation Analysis: In this step, a correlation matrix is computed to display the correlation coefficients (using Pearson's correlation) between every pair of features. These coefficients range from -1 to +1, where +1 indicates a perfect positive correlation (linear function increases, the other increases), -1 indicates a perfect negative correlation (linear function as one variable increases, the other decreases) and 0 means no correlation. Figure 20 shows the correlation matrix that highlights the relationships between all features. Strong correlations (e.g., > 0.8) suggest that two features share a similar pattern or capture similar information. For instance, sand content and clay content are highly negatively correlated (since they represent complementary soil textures), keeping both would be redundant.

- **The final selected features are listed below:**

- Resistivity
- Soil to pipe potential
- Redox potential
- pH
- Potassium content
- SDT
- Iron content
- Sulphate ion content
- Calcium carbonate content
- Sand content
- Silt content
- Bulk density of soil
- Coarse fragment content
- NDVI
- Average rainfall
- Elevation

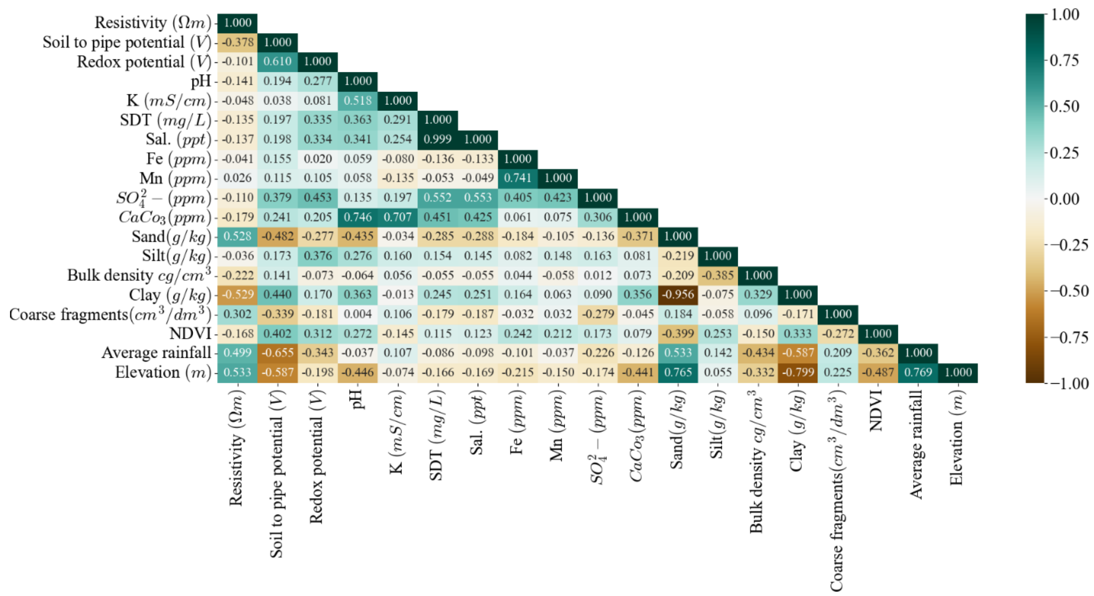

- Figure 20: Feature correlation matrix

3. Dimensionality Reduction: Principal Component Analysis (PCA) is a technique used to reduce the dimensionality of large datasets while retaining the maximum variance (information) from the original data. This method is useful when dealing with many features that may be redundant or less impactful in explaining the underlying patterns in the data. PCA transforms the original features into a new set of uncorrelated variables called principal components (PCs). Each principal component is a linear combination of the original features, and they are ranked by the amount of variance they explain. The first

principal component captures the most variance, the second captures the second most, and so on. Figure 21 shows the scree plot of the percentage explained variance for each component. The goal of PCA is to retain only the components that explain the majority of the variance in the data, typically aiming for 95% or higher cumulative variance. By doing this, the less informative components—those contributing little to the overall variance—can be discarded without losing valuable information. Figure 22 displays a cumulative explained variance plot, showing how the total variance captured increases as more components are included. Based on this plot, the appropriate number of principal components to retain is determined, simplifying the dataset while maintaining the key patterns relevant to the corrosion study. By combining correlation analysis and PCA, the feature selection process becomes more efficient and robust, leading to a cleaner, more interpretable model with better predictive power.

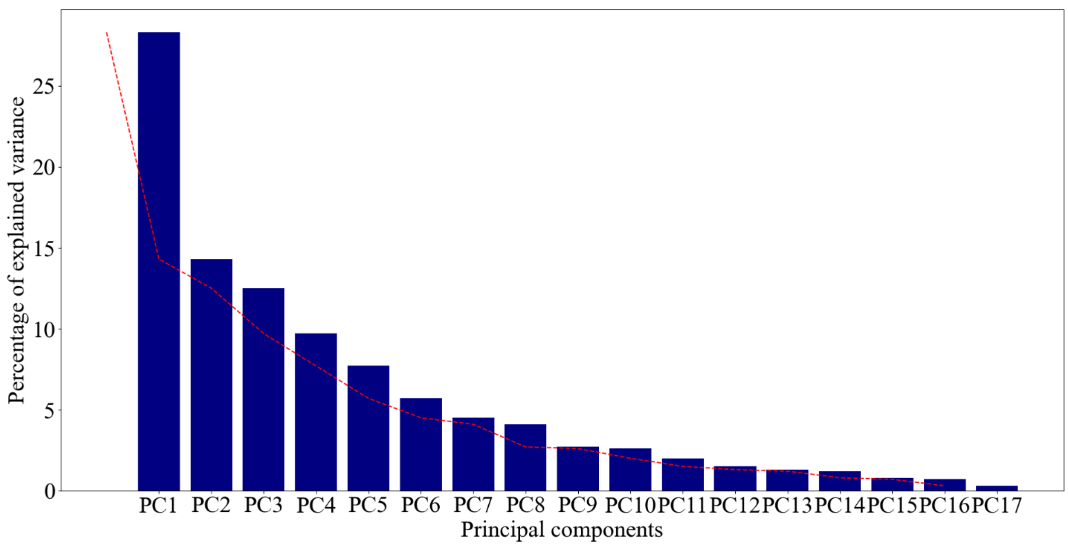

- Figure 21: Scree plot of percentage explained variance for each component

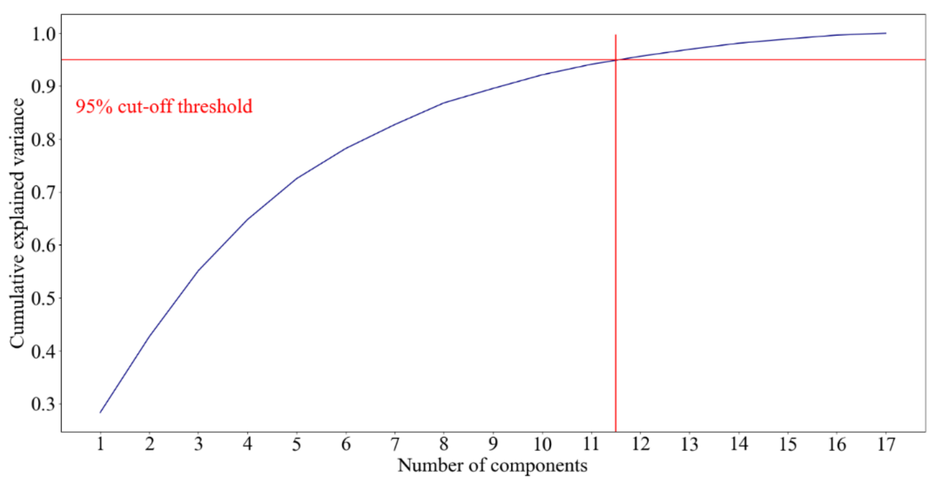

- Figure 22: Cumulative explained variance vs number of components.

- From the analysis above, we see a total number of 11 principle components can be extracted to effectively explain the variation of the original selected features. In the following months, we will start to explore the inherent heterogeneity of the database and identify multiple sections with similar corrosion environments so that the CP effectiveness can be investigated for each condition.

5. Future work

- Continue to update the model with various impedance definitions based on mechanistic analysis of processes occurring at the interface
- Adapt the model for comparison with field data
- Continue EIS testing and building a database of impedance responses of various systems.
    - Instantaneous EIS vs time-based EIS at OCP.
    - Effect of coating thickness with and without defects
    - CP testing under all coating conditions and coating types
- Continue to characterize the potential decay for the various systems.
- Create testing protocol and testing matrix for characterizing various defect geometries and types with reflectometry

References

1. Huang, V.M.-W., et al., *The apparent constant-phase-element behavior of an ideally polarized blocking electrode: a global and local impedance analysis.* Journal of the Electrochemical Society, 2006. **154**(2): p. C81.

2. Brug, G., et al., *The analysis of electrode impedances complicated by the presence of a constant phase element.* Journal of electroanalytical chemistry and interfacial electrochemistry, 1984. **176**(1-2): p. 275-295.

3. Tsai, Y.-T. and D. Whitmore, *Nonlinear least-squares analyses of complex impedance and admittance data for solid electrolytes.* Solid state ionics, 1982. **7**(2): p. 129-139.

4. Marquardt, D.W., *An algorithm for least-squares estimation of nonlinear parameters.* Journal of the society for Industrial and Applied Mathematics, 1963. **11**(2): p. 431-441.

5. Alper, J.S. and R.I. Gelb, *Standard errors and confidence intervals in nonlinear regression: comparison of Monte Carlo and parametric statistics.* Journal of Physical Chemistry, 1990. **94**(11): p. 4747-4751.

6. Boukamp, B.A., *A nonlinear least squares fit procedure for analysis of immittance data of electrochemical systems.* Solid state ionics, 1986. **20**(1): p. 31-44.

7. Macdonald, J.R. and J. Garber, *Analysis of impedance and admittance data for solids and liquids.* Journal of the Electrochemical Society, 1977. **124**(7): p. 1022.

8. Sheppard, R., B. Jordan, and E. Grant, *Least squares analysis of complex data with applications to permittivity measurements.* Journal of Physics D: Applied Physics, 1970. **3**(11): p. 1759.

9. Gadala, I.M. and A. Alfantazi, *Electrochemical behavior of API-X100 pipeline steel in NS4, near-neutral, and mildly alkaline pH simulated soil solutions.* Corrosion Science, 2014. **82**: p. 45-57.